Toxicity of Tungsten Carbide and Cobalt-Doped Tungsten Carbide Nanoparticles in Mammalian Cells *in Vitro*

Susanne Bastian,[1*] Wibke Busch,[2*] Dana Kühnel,[2*] Armin Springer,[3*] Tobias Meißner,[4*] Roland Holke,[4*] Stefan Scholz,[2] Maria Iwe,[1] Wolfgang Pompe,[3] Michael Gelinsky,[3] Annegret Potthoff,[4] Volkmar Richter,[4**] Chrysanthy Ikonomidou,[1**] and Kristin Schirmer[2,5**]

[1]Department of Pediatric Neurology, University Children's Hospital Carl Gustav Carus, University of Technology Dresden, Dresden, Germany; [2]Department of Cell Toxicology, UFZ-Helmholtz Centre for Environmental Research, Leipzig, Germany; [3]Max Bergmann Center of Biomaterials, Institute of Materials Science, University of Technology Dresden, Dresden, Germany; [4]Fraunhofer Institute for Ceramic Technologies and Systems, Dresden, Germany; [5]Eawag, Swiss Federal Institute of Aquatic Science and Technology, Dübendorf, Switzerland

Background: Tungsten carbide nanoparticles are being explored for their use in the manufacture of hard metals. To develop nanoparticles for broad applications, potential risks to human health and the environment should be evaluated and taken into consideration.

Objective: We aimed to assess the toxicity of well-characterized tungsten carbide (WC) and cobalt-doped tungsten carbide (WC-Co) nanoparticle suspensions in an array of mammalian cells.

Methods: We examined acute toxicity of WC and of WC-Co (10% weight content Co) nanoparticles in different human cell lines (lung, skin, and colon) as well as in rat neuronal and glial cells (i.e., primary neuronal and astroglial cultures and the oligodendrocyte precursor cell line OLN-93). Furthermore, using electron microscopy, we assessed whether nanoparticles can be taken up by living cells. We chose these *in vitro* systems in order to evaluate for potential toxicity of the nanoparticles in different mammalian organs (i.e., lung, skin, intestine, and brain).

Results: Chemical–physical characterization confirmed that WC as well as WC-Co nanoparticles with a mean particle size of 145 nm form stable suspensions in serum-containing cell culture media. WC nanoparticles were not acutely toxic to the studied cell lines. However, cytotoxicity became apparent when particles were doped with Co. The most sensitive were astrocytes and colon epithelial cells. Cytotoxicity of WC-Co nanoparticles was higher than expected based on the ionic Co content of the particles. Analysis by electron microscopy demonstrated presence of WC nanoparticles within mammalian cells.

Conclusions: Our findings demonstrate that doping of WC nanoparticles with Co markedly increases their cytotoxic effect and that the presence of WC-Co in particulate form is essential to elicit this combinatorial effect.

Key words: cellular uptake, cobalt doping, cobalt salt, human cell cultures, *in vitro*, nanoparticle behavior, toxicity, tungsten carbide nanoparticles. *Environ Health Perspect* 117:530–536 (2009). doi:10.1289/ehp.0800121 available via *http://dx.doi.org/* [Online 1 December 2008]

Nanotoxicology is an emerging field of research at the intersection of material science, medicine, and toxicology. The ultimate characteristic of nanomaterials is their size, which can modify the physicochemical properties of the material, enable increased uptake and interaction with biological tissues, and generate adverse biological effects in living cells that would not be possible with the same material in larger or soluble form. Smaller particle size leads to increased surface area and allows for a greater proportion of atoms or molecules to be displayed on the surface. Clinical and experimental studies indicate that a small size, a large surface area, and the ability to generate reactive oxygen species (ROS) contribute to the potential of nanoparticles to induce cell injury (Colvin 2003; Nel et al. 2006; Oberdörster et al. 2005).

Most toxicology data for engineered nanomaterials are derived from inhalation studies concentrating on lung injury and assessment of inflammatory parameters. Uptake of metal oxide nanoparticles in lung cells has been demonstrated *in vivo* as well as in different cell culture systems (Geiser et al. 2008; Limbach et al. 2005; Stearns et al. 2001). Toxic effects in human lung cells depend on particle composition and size and related reactivity (Brunner et al. 2006; Duffin et al. 2007; Limbach et al. 2005, 2007). So-called nanoeffects, meaning differing effects of nanomaterials compared with bulk materials of the same chemical composition, have been observed, with nanomaterials being more toxic in regard to reduction of cell viability or induction of oxidative stress and inflammatory mediators (Wörle-Knirsch et al. 2007; Zhang et al. 2000, 2003).

Tungsten carbide (WC) nanoparticles are now being considered for the manufacture of hard metals to achieve extreme hardness and wear resistance, and mixing with cobalt is thought to improve toughness and strength of the material. In the past, occupational exposure to Co-containing dust in production facilities, which generally falls in the 1–20 μm size range (Stefaniak et al. 2008), has been associated with bronchial asthma, fibrosing alveolitis, and lung cancer (Lison 1996; Moulin et al. 1998). Tungsten carbide–Co (WC-Co) hard metal is now classified by the International Agency for Research on Cancer (IARC) as probably carcinogenic to humans, based on limited evidence in humans and sufficient evidence in experimental animals (IARC 2006). Experimental work has shown a higher mutagenic potential of the WC-Co mixture compared with its individual components (van Goethem et al. 1997), a finding that has been attributed to increased production of ROS. WC-Co exposure of peripheral blood mononucleated cells has been shown to trigger apoptosis of these cells via a caspase-9–dependent pathway (Lombaert et al. 2004) and to generally up-regulate apoptotic and stress/defense response pathways (Lombaert et al. 2008). Ultrastructural analysis revealed that WC particles are incorporated into numerous vacuoles, whereas WC-Co particles lead to lysis of the cells, and no structural alterations due to Co particles could be demonstrated (Lison and Lauwerys 1990). Extensive studies on genotoxicity and mutagenicity have been conducted after a series of epidemiologic studies showed that hard-metal workers exposed to airborne WC and Co dust in occupational settings have increased mortality from lung cancer (Moulin et al. 1998).

Little information exists regarding effects of nanoparticles on other potentially exposed organs (i.e., skin, intestine, and the nervous system), although systemic circulation and distribution of inhaled or injected nanoparticles to different organs have been reported (Kreyling et al. 2002; Nemmar et al. 2001, 2002; Takenaka et al. 2001). Nanoparticles may translocate to the central nervous

Address correspondence to K. Schirmer, Environmental Toxicology, Eawag, Überlandstrasse 133, 8600 Dübendorf, Switzerland. Telephone: 41-0-44-823-5266. Fax: 41-0-44-823-5311. E-mail: kristin.schirmer@eawag.ch

*These authors contributed equally to this article.
**These authors contributed equally to this article.

Supplemental Material is available online at http://www.ehponline.org/members/2008/0800121/suppl.pdf

This research was supported by the German Federal Ministry for Education and Research within the project Identifizierung und Bewertung von Gesundheits- und Umweltauswirkungen von technischen nanoskaligen Partikeln (grant 03X0013C).

The authors declare they have no competing financial interests.

Received 22 August 2008; accepted 1 December 2008.

system via the olfactory nerve (Oberdörster et al. 2005). A few neurotoxicologic studies have shown that titanium dioxide nanoparticles accumulate in microglial cells, causing increased ROS production, mitochondrial swelling, and membrane disruption (Long et al. 2006). Pisanic et al. (2007) reported reduction of neurite outgrowth and formation of intercellular connections after exposure of neurons to iron oxide nanoparticles.

In this study, we evaluated acute toxicity of WC and WC-Co nanoparticles in *in vitro* systems (i.e., human epithelial and rat neuronal and glial cells). Here we report the physicochemical characterization of WC and WC-Co nanoparticles in cell culture media and describe their intracellular distribution and cytotoxicity profile.

Materials and Methods

Particles. **Preparation.** WC and WC-Co particles (10% weight content of Co) were prepared by a chemical process and deaggregated and mixed, respectively, by means of a ball mill. We milled the nearly pure WC powder and Co powder in a hard-metal–lined ball mill using hard metal balls [see Supplemental Material, "Particle preparation and characterization," and Supplementary Material, Table 1 and Figure 1 (http://www.ehponline.org/members/2008/0800121/suppl.pdf)].

From both types of particles, we prepared suspensions of 100 μg/mL in pure water (resistivity ≥ 18 MΩ·cm; Wilhelm Werner GmbH, Leverkusen, Germany). For WC, water was sufficient to prepare electrostatically stable particle suspensions. For WC-Co, the addition of 0.01% (wt/vol) sodium polyphosphate solution (Graham's salt; CAS no. 10361-03-25; Merck, KGaA, Darmstadt, Germany) was necessary to obtain electrostatic stabilization of the particles, apparently due to the presence of Co. Graham's salt is an often-used dispersant that is nontoxic in the applied concentrations. The suspensions were treated in an ultrasonic bath (RK 255 H; Bandelin, Berlin, Germany) for deagglomeration. After preparation, we quantified particle size and zeta potential. Time-dependent measurements in physiologic media (cell culture media or buffers) were performed by stirring a mixture of 90% (vol/vol) media and 10% (vol/vol) nanoparticle suspension in a beaker. The resulting suspensions were filled in a square cuvette for measurements. In parallel, studies were carried out in phosphate-buffered saline (PBS; Biochrom, Berlin, Germany) with or without bovine serum albumin (BSA; bovine fraction V, CAS no. 9048-46-8; Merck), which was dissolved in PBS before adding the particle suspension. We also performed experiments in Hank's buffered salt solution (HBSS; Biochrom) or Dulbecco's modified Eagle's medium (DMEM; PAA Laboratories, Pasching, Austria) with or without 5% or 10% (vol/vol) fetal bovine serum (FBS; Invitrogen, Karlsruhe, Germany).

Physicochemical characterization. We determined the N_2-BET specific surface area (BET; Brunauer, Emmet, Teller, after the developers of the basic calculations) of WC and WC-Co powders using an ASAP 2010 accelerated surface area and porosimetry analyzer (Micromeritics GmbH, Mönchengladbach, Germany). We determined the particle size distribution using dynamic light scattering (ZetaSizer Nano ZS; Malvern Instruments Ltd., Worcestershire, UK). We analyzed the mean particle size, x_{PCS}, and the polydispersity index (PDI), which are described in DIN ISO 13321 (1996). We calculated the zeta potential from the Smoluchowski equation by measuring the electrophoretic mobility (ZetaSizer Nano ZS). These measurements were taken before and after autoclaving and yielded similar results. Therefore, we chose to sterilize the particle suspensions by autoclaving before exposure of cells. Solubility experiments were performed by centrifuging the nanoparticle suspensions at 15,000 × *g* (Sigma 4K15; Sigma Laborzentrifugen GmbH, Osterode am Harz, Germany). We then used clear supernatant to determine the tungsten and Co concentration using inductively coupled plasma–optical emission spectroscopy (Ultima; HORIBA Jobin Yvon, Unterhaching, Germany).

Preparation of Co and tungsten salt solutions. We prepared cobalt chloride ($CoCl_2$; Fluka/Sigma-Aldrich, Seelze, Germany) and sodium tungstate dihydrate solutions (Sigma) in distilled water at concentrations of 10 mM or 20 mM. Stock solutions were sterilized by autoclaving. We obtained all concentrations used in cell assays by serial dilution of the stock solutions with cell culture grade water (PAA Laboratories) under sterile conditions. Solutions were stored at 4°C.

Cell culture. **Cell lines.** We used the following cell lines: CaCo-2 human colon adenocarcinoma cells [HTB-37; American Type Culture Collection (ATCC), Rockville, MD, USA), HaCaT human keratinocyte cells (CLS Cell Lines Service, Eppelheim, Germany) (Boukamp et al. 1988), A549 human lung carcinoma cells (CCL-185; ATCC), and OLN-93 oligodendroglial precursor cells (provided by the Department of Neonatology, Charité, Berlin, Germany).

Primary neuronal and astroglial cell cultures. Neuronal cell cultures were prepared from cortices of Wistar rat fetuses on gestation day 18 according to Fedoroff and Richardson (1997). Detailed descriptions of the routine maintenance of all applied cell cultures is available in the Supplemental Material ["Cell culture and assessment of cell viability" (http://www.ehponline.org/members/2008/0800121/suppl.pdf)].

Exposure of cells to particles. The CaCo-2, HaCaT, and A549 cells were plated at a density of 5×10^4 cells/well in a final volume of 500 μL in 24-well plates (Techno Plastic Products AG, Trasadingen, Switzerland) and allowed to attach for 24 hr before addition of particle suspensions. We then added 50 μL of the respective dilution of the particle suspension to 450 μL complete cell culture medium to reach final concentrations of 7.5, 15, and 30 μg/mL for WC nanoparticles and 8.25, 16.5, and 33 μg/mL for WC-Co nanoparticles. The water used to prepare the particle suspension (with or without Graham's salt) was included as a control (vehicle).

We exposed cells to nanoparticle-containing solutions or vehicle control for 1 hr to 3 days. For exposure of cells with $CoCl_2$ or sodium tungstate dihydrate, we added a maximal volume of 10% (vol/vol) salt solution to cell culture medium to reach the desired final concentrations. For coexposure of $CoCl_2$ and WC, we added 5% (vol/vol) $CoCl_2$ and 5% (vol/vol) of WC suspension to the cell culture medium to reach the same final concentrations of $CoCl_2$ and 15 μg/mL WC.

We plated OLN-93 cells (1×10^4 cells/mL) and primary cells (5×10^4 cells/mL) in 96-multiwell plates in a final volume of 100 μL (Greiner Bio-One, Frickenhausen, Germany) and allowed them to attach for at least 24 hr before adding particle suspension. We added particle dilutions as described above, and cells were exposed for 3 days.

Electron microscopy. For scanning electron microscopy (SEM) of cells, harvested cells were fixed with 2% (vol/vol) glutaraldehyde (Serva, Heidelberg, Germany) at room temperature, postfixed with 1% (vol/vol) osmium tetroxide (Roth, Karlsruhe, Germany), dehydrated in a graded series of acetone [including a staining step with 1% (vol/vol) uranyl acetate], and embedded in epoxy resin according to Spurr (1969). To avoid interference of the uranyl acetate and osmium tetroxide during energy-dispersive X-ray spectroscopy (EDX), we did not stain respective samples with the heavy metals; these samples were fixed in 2% (vol/vol) glutaraldehyde, dehydrated, and embedded in epoxy resin as above. Samples were cut on a Leica EM UC6 ultramicrotome (Leica, Vienna, Austria), equipped with a diamond knife (Diatome, Biel, Switzerland), carbon coated, and analyzed using a Philips XL 30 ESEM (Philips, Eindhoven, Netherlands). For EDX analyses, we used an EDAX detecting unit and EDAX software (version 3.0; EDAX Inc., Mahwah, NJ, USA).

Assessment of cell viability. **Light microscopy.** Before termination of exposure, we observed cells by light microscopy using an inverse microscope.

Assays for cell viability. We determined cell viability using fluorescent indicator

dyes that measure cellular metabolic activity [AlamarBlue (Biosource, Nivelle, Belgium) and Cell Counting Kit 8 (CCK-8; Dojindo Laboratories, Kumamoto, Japan)] and cell membrane integrity [5-carboxyfluorescein diacetate, acetoxymethyl ester (CFDA-AM) (Molecular Probes, Eugene, OR, USA)]. We followed procedures described by Schirmer et al. (1997) for AlamarBlue/CFDA-AM and the supplier's protocol for CCK-8. Details of the procedures are provided in the Supplementary Material ["Cell culture and assessment of cell viability" (http://www.ehponline.org/members/2008/0800121/suppl.pdf)].

Table 1. Physical properties of investigated nanoparticles.

Substance	BET (m^2/g)[a]	x_{PCS} (nm)[b]	PDI	Zeta potential (mV)
WC	6.9	145 ± 5	0.2	–35
WC-Co	6.6	145 ± 5	0.2	–50

[a]Specific surface area. [b]Mean particle size.

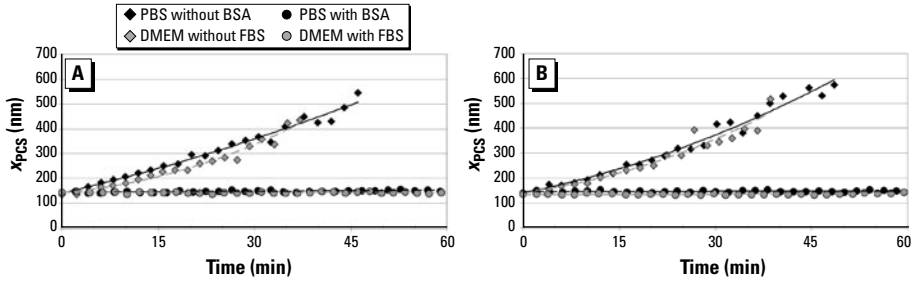

Figure 1. Effect of BSA in PBS and 5% (vol/vol) FBS in DMEM on the stability of the WC (*A*) and WC-Co (*B*) particles (10 µg/mL) compared to protein-free PBS and DMEM. We found identical results for WC and WC-Co in HBSS (data not shown).

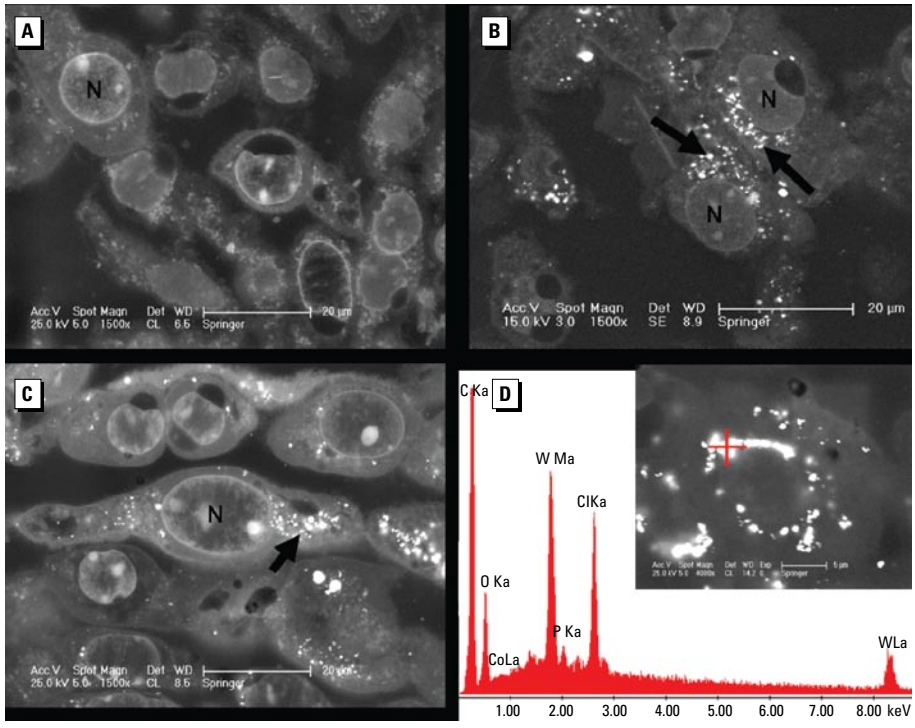

Figure 2. SEM (BSE) of embedded HaCaT cells after 2 days of incubation with medium without particles (*A*; control), 30 µg/mL WC nanoparticles (*B*), or 33 µg/mL WC-Co nanoparticles (*C*). Magnification, 1,500×. Heavy elements (e.g., tungsten and Co) appear as light areas (arrows in *B* and *C*), which are concentrated within the cytoplasm [gray regions around the nuclei (N)] but not inside the nuclei. (*D*) EDX analysis of the region indicated by a cross in the inset. We used the same conditions as for (*C*) (incubation with 33 µg/mL WC-Co particles for 2 days) but the sample was prepared without heavy metal staining. The spectrum shows two prominent X-ray peaks with the characteristic energy for X-ray quants originating from the W-M_α (W Ma) and W-L_α (W La) atomic shells, respectively. Other peaks represent further elements in the measured area and are due to compounds of the embedding media (ClKa, chloride K_a; O Ka, oxygen K_a), coating (C Ka, carbon K_a), or compounds of the cell (P Ka, phosphorus K_a; C, O). The Co-L_α (CoLa) peak of WC-Co is below the detection threshold.

Statistics. Exposure experiments with cells were performed in quadruplicate wells in three independent tests. We analyzed statistical differences using one-way analysis of variance (ANOVA) followed by Dunnett's posttest (treatments vs. control), Tukey's posttest (treatment vs. treatment), or two-way ANOVA followed by Bonferroni posttest using GraphPad Prism software (GraphPad Prism version 4.00 for Windows; GraphPad Software, Inc., San Diego, CA, USA). We considered *p*-values < 0.05 to be statistically significant. Fluorescence/absorbance units obtained in the cell viability assays were converted to percent of control and are presented as mean ± SD.

Results

Particles. **Initial characteristics.** The obtained BET specific surface area was 6.9 m^2/g for WC and 6.6 m^2/g for WC-Co. We expected the similarity in BET because WC-Co consists of 90% weight WC powder and both were milled under equal conditions. The particle size distribution and the morphology also were nearly the same, which we confirmed by two independent methods: SEM and dynamic light scattering. The mean particle size, x_{PCS}, which formed the initial value for studying the time dependence of agglomeration, was 145 ± 5 nm in both cases. The PDIs of 0.2 indicated a rather broad size range. We calculated the particle size range to be between 50 and 300 nm [see Supplemental Material, Figure 2 (http://www.ehponline.org/members/2008/0800121/suppl.pdf)]. The measured zeta potentials were approximately –35 mV for WC in water and –50 mV for WC-Co in sodium polyphosphate stabilized suspension. The high absolute values of the zeta potentials ensure a stable suspension in both cases because of the strength of the electrostatic repulsion force. Table 1 summarizes the physical parameters of both materials.

Dispersion stability in physiologic media. WC and WC-Co particles undergo agglomeration after addition to a protein-free physiologic medium. We studied the influence of different physiologic media (PBS, HBSS, DMEM) on agglomeration but found no differences. Likewise, we found no significant difference in the agglomeration behavior between WC and WC-Co particles. The absolute value of the zeta potential decreased after addition of the particles to PBS, HBSS, or DMEM. Zeta potentials for WC and WC-Co were between –20 and –23 mV.

In contrast to protein-free media, experiments with the protein albumin (BSA) in PBS showed no agglomeration of WC and WC-Co particles. Measured zeta potentials of the BSA-coated particles were about –11 mV. Although this small absolute value stands for a low electrostatic repulsion force, a steric component of the protein appears to lead to a stabilizing effect. To go one step further, we

performed these investigations in DMEM or HBSS with 5% or 10% (vol/vol) serum to have the same conditions as in the cell culture experiments. There, we achieved the same stabilization effect for both serum concentrations. As already described for WC/WC-Co in PBS with BSA, the zeta potential of the particles in DMEM or HBSS with FBS was –11 mV. Figure 1 shows examples of the behavior of the particles in DMEM and PBS.

We determined the tendency of the particles to dissolve after we allowed the stock suspensions to stand for 1 week. For WC, 6% of the tungsten dissolved. For WC-Co, 15% of the tungsten and 76% of the Co dissolved. This level of dissolution of Co^{2+} from WC-Co is similar to that reported by Lombaert et al. (2004) for microsized WC-Co.

Uptake of particles by cells. To investigate whether WC or WC-Co nanoparticles are able to enter cells, we incubated HaCaT cells for 2 days with 30 µg/mL WC or 33 µg/mL WC-Co particles, respectively (Figure 2). Examination by SEM [back-scattered electron detector (BSE)] of epoxy-resin–embedded samples showed that particles and/or agglomerates with strong BSE signals were detectable in cells treated with WC particles (Figure 2B) and WC-Co particles (Figure 2C) but not in the control group (Figure 2A). Furthermore, the BSE signals of the particles/agglomerates are visible within the cells, but no agglomerates or particles were detectable inside the nucleus. Additional elemental analysis with EDX of one of the strong BSE signals caused by particles/agglomerates revealed an X-ray energy peak that exclusively belonged to tungsten, thereby indicating WC (or WC-Co; Figure 2D). These observations clearly confirm that nano-sized WC and WC-Co particles (or agglomerates) are able to enter cells. We likewise observed this for a series of other cells, including lung cells (A549) and oligodendrocytes (OLN-93; data not shown).

Impact on cell viability. **Particles.** WC nanoparticles did not yield a toxic response up to 30 µg/mL after 3 days of exposure in either of the human epithelial cell lines, the OLN-93 cell line, or the primary rat neuronal and astroglial cells (Figures 3 and 4). Exposure of the cell cultures to WC-Co elicited slight to substantial toxicity, with the order of sensitivity being primary astrocytes > intestinal cells (CaCo-2) > oligodendrocytes (OLN-93) > skin cells (HaCaT) > lung cells (A549) > primary neuronal cells (Figures 3 and 4). Comparison of the sensitivity of each cell line to WC and WC-Co particles over the tested concentration range by means of two-way ANOVA revealed that the addition of Co significantly increased toxicity of the particles for intestinal and skin epithelial cells as well as gliotoxicity (toxicity to astrocytes and oligodendrocytes).

Role of Co ions in toxicity. To investigate whether the Co fraction of WC-Co alone accounts for the toxic effects, we performed experiments using $CoCl_2$. We found decreased viability of cells treated with $CoCl_2$ starting from a concentration of 100 µM for the human cell lines (Figure 5). For comparison, the maximum Co concentration in the highest tested WC-Co particle concentration (33 µg/mL) is 51 µM. When cells were exposed to this Co concentration together with WC particles, we likewise did not observe toxicity (Figure 5, insets). We concluded that the Co fraction in the WC-Co particles alone could not account for the toxicity observed after treatment with WC-Co and that it is the combination of the particulate WC with Co that causes the cytotoxic effect (Figure 5, insets). We obtained similar results for the oligodendroglial cell line OLN-93 (data not shown).

Role of tungsten ions in toxicity. We tested tungsten salt ($Na_2WO_4 \cdot 2H_2O$) for its toxicity in OLN-93 cells and in astrocytes. We found no cytotoxicity of tungstate at the concentrations of 14, 28, and 42 µM, which correspond to 9%, 18%, and 28% dissolved tungsten. Cytotoxicity became apparent only at tungsten salt concentrations > 250 µM, which exceeds the level of tungsten present in any of the particle exposure experiments [for an example, see Supplemental Material, Figure 3 (http://www.ehponline.org/members/2008/0800121/suppl.pdf)].

Discussion

Here we show that WC-Co nanoparticles can be toxic to mammalian epithelial, neuronal, and glial cells, whereas we detected no significant acute toxicity of WC nanoparticles in our test systems. Chemical–physical characterization confirmed that WC as well as WC-Co nanoparticles with an average diameter of 145 nm form a stable suspension in buffers that contain albumin and in cell culture media that contain serum. Cytotoxicity seen with WC-Co nanoparticles was higher than

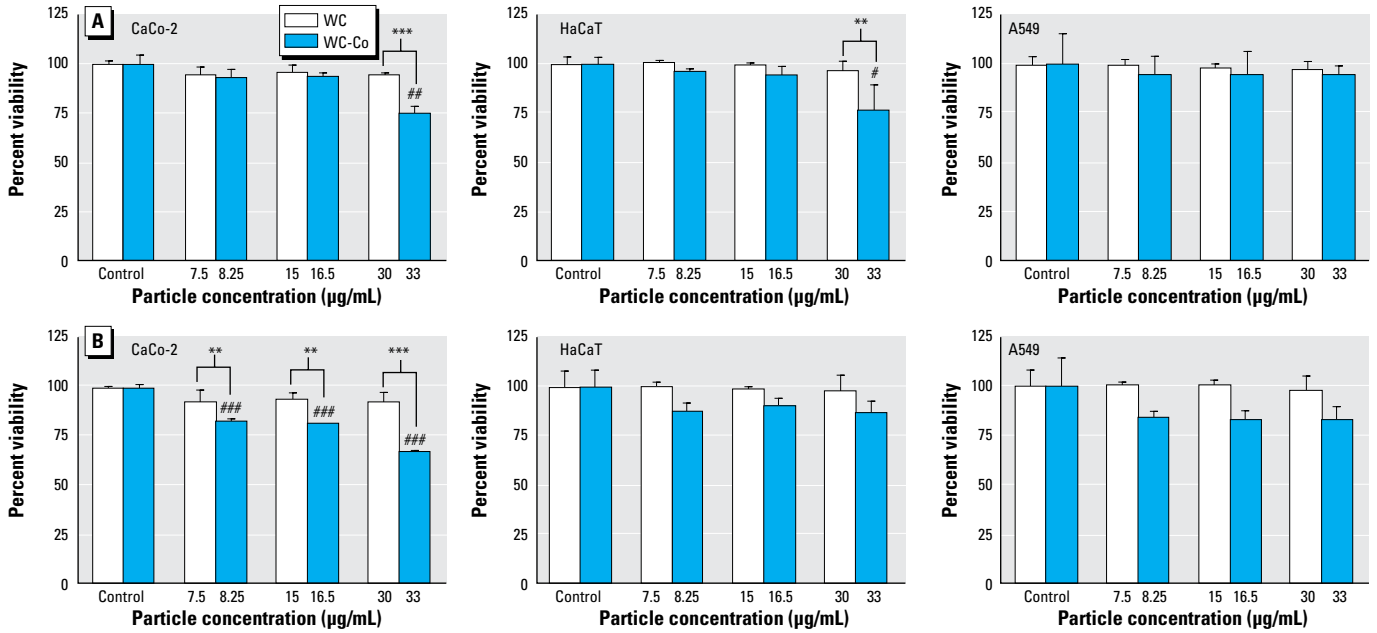

Figure 3. Cell viability, measured as metabolic activity with AlamarBlue (*A*) and as membrane integrity with CFDA-AM (*B*), of three human cell lines [CaCo-2 (left) HaCaT (center) or A549 (right)] after exposure for 3 days to WC-Co or WC. Results are expressed as a percentage of control cells that received identical treatment but without particles (mean ± SD; $n = 3$).

$^{\#}p < 0.05$, $^{\#\#}p < 0.01$, and $^{\#\#\#}p < 0.001$ compared with control by one-way ANOVA with Dunnett's posttest. $^{**}p < 0.01$, and $^{***}p < 0.001$ by two-way ANOVA with Bonferroni posttest comparing both particle types. In (*B*), HaCaT cells showed overall treatment significance at $p < 0.01$ by two-way ANOVA.

expected based on ionic Co content, indicating a qualitative cytotoxic effect of nano-sized particulate matter. Analysis by electron microscopy demonstrated the presence of WC nanoparticles within exposed mammalian cells.

Most of the chemical and physical parameters of WC and WC-Co nanoparticles are similar. Initial physical properties (x_{PCS}, PDI, BET) and the behavior in the physiologic media are identical. Both nanoparticles show similar agglomeration kinetics in all tested physiologic media. Furthermore, agglomeration of the nanoparticles can be inhibited in the presence of BSA or FBS. Obviously, the protein BSA adsorbs on the particle surface and stabilizes the suspension (Cedervall et al. 2007; Schulze et al. 2008). This result is comparable with stabilization of fullerene (C_{60}) nanoparticles in PBS induced by human serum albumin (Deguchi et al. 2007). This stabilizing effect seems to apply to chemically different nanoparticles. Whereas fullerene is a special carbon modification, WC is a nonoxide ceramic.

Ultrastructural analysis by electron microscopy revealed the presence of WC particles within exposed cells. The examination of the epoxy-resin–embedded samples with different SEM methods (BSE detector signal, EDX analysis) enabled us to identify both the position and the chemical composition of the particles within the cells. The absence of the peak for Co in the EDX spectra may be explained by the low amount [only 10% (wt/wt) Co in WC-Co] and its tendency to dissolve. The lack of a Co peak may also be an example of possible artifacts that result from the extensive washing steps within the embedding procedure, which can reduce the EDX signal of Co below the detection threshold of the EDX detector. Nevertheless, the observations clearly confirm that nano-sized WC and WC-Co particles (or agglomerates thereof) are able to enter the cells. According to our findings, WC and WC-Co particles do not penetrate the nuclear membrane, because we detected no nanoparticles within the nuclei. It is, however, possible that particles with a size below the resolution of the SEM (therefore undetectable) can pass through the nuclear membrane. So far, we are not able to propose a mechanism for uptake of nano-sized WC or WC-Co particles or agglomerates based on the SEM and EDX data shown here. Endocytosis is a possibility. Stearns et al. (2001) documented this mechanism for uptake of ultrafine titanium dioxide particles by A549 lung cells. In contrast to the studies by Lison and Lauwerys (1990), who observed uptake of micro-sized (1–4 μm)

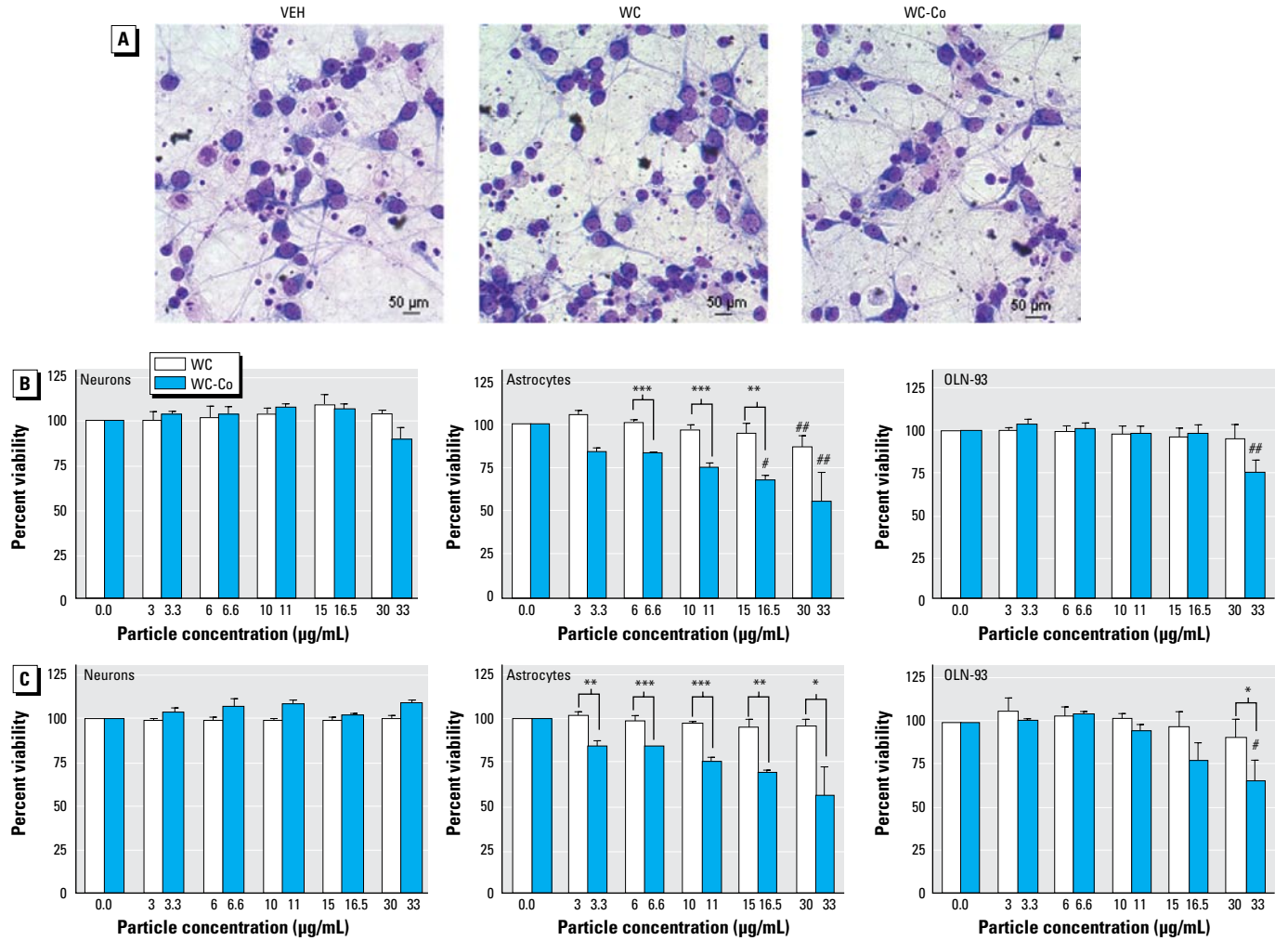

Figure 4. Effects of WC and WC-Co on cultured rat brain cells. (*A*) Light micrographs of neuronal cultures stained with Giemsa after a 72-hr exposure to vehicle (VEH; aqueous media used for particle preparations), WC particles (10 μg/mL), or WC-Co particles (11 μg/mL); there is no apparent difference in the appearance of the cultured neurons. (*B–C*) Cell viability of primary neuronal (left) and astroglial (center) cultures and the oligodendroglial cell line OLN-93 (right) after exposure to WC and WC-Co particles over 3 days measured by the CCK-8 assay (*B*) or AlamarBlue (*C*). WC particles caused a small but significant effect on cell viability of astrocytes at the highest concentration; WC-Co particles significantly decreased viability in oligodendrocytes and astrocytes in a concentration-dependent manner. Two way ANOVA revealed that there was a significantly higher toxicity of WC-Co particles in astrocytes and OLN-93 cells compared with WC particles. Results are expressed as a percentage of control values (mean ± SD; $n = 3–6$).

$^{\#}p < 0.05$; $^{\#\#}p < 0.01$; and $^{\#\#\#}p < 0.001$ compared with control by one-way ANOVA with Dunnett's posttest. $^{*}p < 0.05$; $^{**}p < 0.01$; and $^{***}p < 0.001$ comparing both particle types by two-way ANOVA with Bonferroni posttest.

WC and WC-Co particles by mouse peritoneal and rat alveolar macrophages, the mammalian cells used here and by Stearns et al. (2001) are not primarily phagocytic cells.

Nano-sized WC-Co particles, but not Co or tungsten ions at concentrations equivalent to the particulate form, or WC nanoparticles alone, led to acute toxicity in most of the cell cultures studied. The fact that the enhanced toxicity occurred only for WC-Co nanoparticles and not for WC particles with added Co^{2+} underlines the role of the particulate form for the expression of toxicity. An enhanced cytotoxicity of WC-Co was first reported by Lison and Lauwerys (1990) based on micro-sized dust in macrophage cells and was likewise shown to depend on the particulate form of the WC-Co mixture (Lison and Lauwerys 1992). In light of the genotoxic and carcinogenic potential of Co-containing hard metal particles and free Co^{2+} ions (Beyersmann and Hartwig 2008; Lison et al. 2001), and the current efforts to improve material designs based on WC-Co nanostructures, further studies are warranted to investigate whether nano-level WC-Co particles elicit size-specific toxic effects.

The mechanism behind the increase in toxicity for nano-sized WC-Co particles is not yet understood, but experiments with hard metal alloys suggested that the association of Co and carbide particles represents a specific toxic entity that produces large amounts of ROS. When both materials in particulate form are in close contact, electrons are transferred from Co to the surface of WC. This process leads to the production of activated (reduced) oxygen, and subsequently, oxidized Co (Co^{2+}) passes into solution (Gries and Prakash 2007; Lison et al. 1995). The additional toxic effect of WC-Co may then be due to a combination of two known mechanisms of Co toxicity: cell damage induced by ROS derived from metallic Co (Hoet et al. 2002), and subsequent inhibition of DNA repair mechanisms by the Co^{2+} ions generated in this process (Kasten et al. 1997). In the rat, acute lung toxicity of a mixture of WC and Co was more pronounced than toxicity of individual components. The amount of excreted Co was higher in WC-Co–exposed animals compared with an equivalent amount of Co. This may be due to an increased bioavailability of Co from WC-Co (Lasfargues et al. 1992).

For nano-sized particles, however, an additional mechanism proposed by Limbach et al. (2007) may be relevant. They suggested a "Trojan horse"-like uptake of toxic ion with the metallic nanoparticle acting as carrier. In cases of toxic ions, the particle helps to cross the cell membrane barrier, thereby enhancing toxicity of the material because the damaging agent is delivered directly into the cell. This mechanism is likely to be involved with WC-Co–mediated toxicity, because a 3-fold higher Co uptake from the WC-Co mixture compared with Co metal powder alone could be demonstrated (Lison and Lauwerys 1990).

In the *in vitro* experiments, we observed that acute toxicity of WC-Co nanoparticles differed depending on the cell culture systems. Most sensitive were astrocytes and colon epithelial cells. Oligodendrocytes, human keratinocytes, and lung epithelial cells showed decreased viability at the highest concentration of WC-Co applied. Interestingly, neurons were resistant to acute application of WC or WC-Co nanoparticles. Little is known so far about the differential sensitivity of the cell lines, for example, with regard to oxidative stress. However, the CaCo-2 cell line appeared more vulnerable to oxidative stress and DNA damage due to a cyanobacterial toxin than were a human astrocytoma and a human B-lymphoblastoid cell line (Zegura et al. 2008). Differences in sensitivity of brain cells to oxidative stress have also been reported. Feeney et al. (2008) used organotypic hippocampal slices to study toxicity of hydrogen peroxide and found that astrocytes were more sensitive to oxidative stress than were neurons. In addition, Dringen et al. (2005) compared peroxide metabolism in cultured brain cells (astrocytes, oligodendrocytes, microglia, and neurons) and found that cultured oligodendrocytes disposed of the peroxide quicker than did the other neural and glial cell cultures. These findings suggest that different brain cells show variable efficiency in dealing with oxidative stress, with the observed

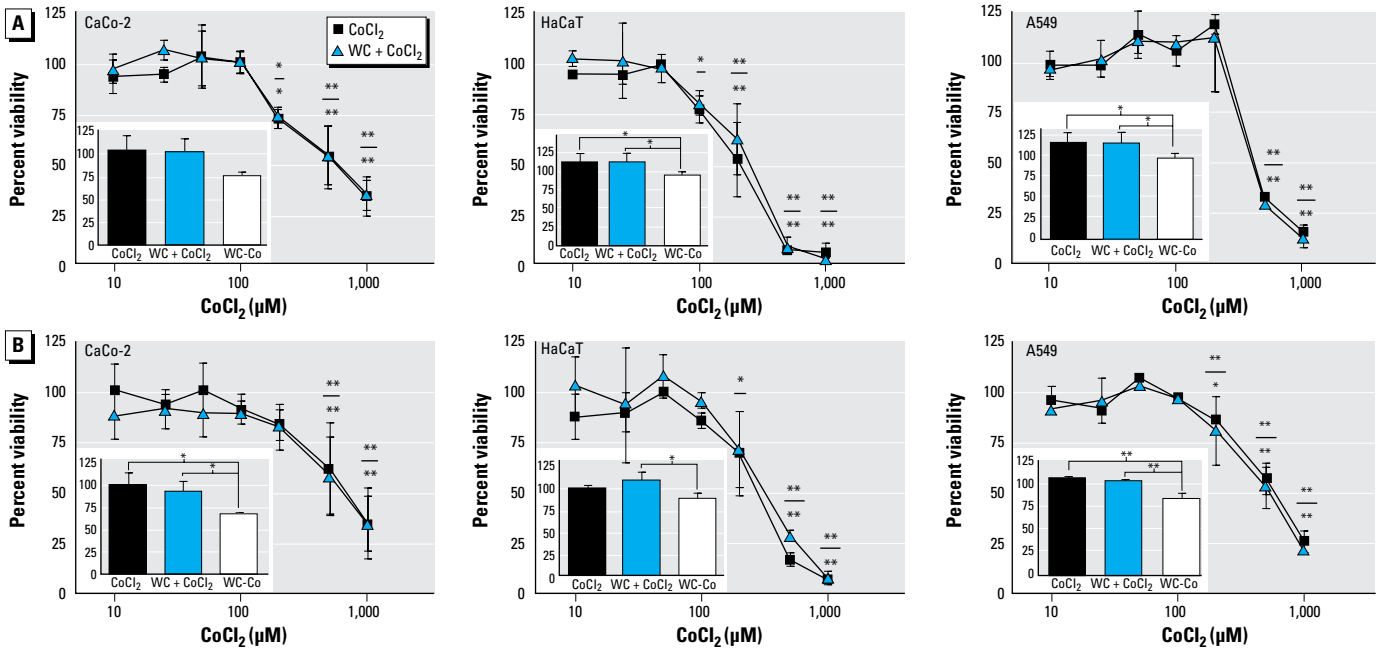

Figure 5. Cell viability (mean ± SD; $n = 3$), measured as metabolic activity with AlamarBlue (*A*) and as membrane integrity with CFDA-AM (*B*), of three human cell lines [CaCo-2 (left), HaCaT (center), and A549 (right)] is concentration-dependently decreased at ≥ 100 μM of $CoCl_2$ after 3 days of exposure; addition of WC particles (15 μg/mL) did not alter these effects. Results are expressed as a percentage of control cells that received identical treatments but not Co or particles ($n = 3$). Insets show that WC-Co particles [33 μg/mL; maximum Co content of 51 μM (equal 10% wt/wt, or 3 μg/mL)] were significantly more potent in affecting cell viability than was $CoCl_2$ (50 μM) or $CoCl_2$ (50 μM) + WC (15 μg/mL). All cells were treated with the same total amount of Co. Cell viability is decreased in all cells that were exposed to WC-Co compared with cells exposed to either $CoCl_2$ or WC + $CoCl_2$.

In (*A*),*$p < 0.05$; and **$p < 0.01$ compared with control by one-way ANOVA followed by Dunnett's posttest. In (*B*),*$p < 0.05$; and **$p < 0.01$, between treatments by one-way ANOVA followed by Turkey's posttest.

susceptibilities conforming with the results of our study, which demonstrate that astrocytes are the most vulnerable brain cells to toxicity of WC-Co. These results indicate that vulnerability of different tissues to WC-Co nanoparticles will differ *in vivo*, as well. If WC-Co nanoparticles were to reach all organs to an equal extent, the highest toxicity would be expected within the nervous system because astrocytes were most vulnerable. Although neurons were not susceptible to acute toxicity of WC-Co nanoparticles, ongoing studies suggest that neurons react with increased production of ROS (data not shown). Thus, although we did not observe acute neuronal loss, it is possible that chronic exposure of neurons, which are nondividing, long-living cells, may eventually result in slow degeneration *in vivo*. Also, because astrocytes were very susceptible and because there is close interaction between astrocytes and neurons within the brain, secondary effects in neurons can be expected. Particulate matter has been shown to penetrate into the central nervous system of mammals and cause neurodegeneration (Campbell et al. 2005; Peters et al. 2006).

Conclusions

Additional research is needed to evaluate mechanisms of acute toxicity of Co-doped WC nanoparticles in mammalian cells and evaluate biochemical pathways that account for differences in susceptibility of cell types. Our approach of using multiple cell cultures and cytotoxicity end points has proven valuable in revealing the combinatorial nanoparticle-mediated effects important for hazard assessment. An important next step is to take the exposure concentrations *in vitro* and *in vivo* into account to identify whether the potential target sites described by us are indeed prone to significant nanoparticle exposure. *In vivo* toxicology will thus help address whether systemic toxicity and neurotoxicity may occur after exposure to WC-Co.

References

Beyersmann D, Hartwig A. 2008. Carcinogenic metal compounds: recent insight into molecular and cellular mechanisms. Arch Toxicol 82:493–512.

Boukamp P, Petrussevska RT, Breitkreutz D, Hornung J, Markham A, Fusenig NE. 1988. Normal keratinization in a spontaneously immortalized aneuploid human keratinocyte cell line. J Cell Biol 106:761–771.

Brunner TJ, Wick P, Manser P, Spohn P, Grass RN, Limbach LK, et al. 2006. In vitro cytotoxicity of oxide nanoparticles: comparison to asbestos, silica, and the effect of particle solubility. Environ Sci Technol 40:4374–4381.

Campbell A, Oldham M, Becaria A, Bondy SC, Meacher D, Sioutas C, et al. 2005. Particulate matter in polluted air may increase biomarkers of inflammation in mouse brain. Neurotoxicology 26:133–140.

Cedervall T, Lynch I, Lindman S, Berggard T, Thulin E, Nilsson H, et al. 2007. Understanding the nanoparticle-protein corona using methods to quantify exchange rates and affinities of proteins for nanoparticles. Proc Natl Acad Sci USA 104:2050–2055.

Colvin VL. 2003. The potential environmental impact of engineered nanomaterials. Nat Biotechnol 21:1166–1170.

Deguchi S, Yamazaki T, Mukai SA, Usami R, Horikoshi K. 2007. Stabilization of C60 nanoparticles by protein adsorption and its implications for toxicity studies. Chem Res Toxicol 20:854–858.

DIN ISO 13321. 1996. Partikelgrößenanalyse – Photonenkorrelationsspektroskopie.

Dringen R, Pawlowski PG, Hirrlinger J. 2005. Peroxide detoxification by brain cells. J Neurosci Res 79:157–165.

Duffin R, Tran L, Brown D, Stone V, Donaldson K. 2007. Proinflammogenic effects of low-toxicity and metal nanoparticles in vivo and in vitro: highlighting the role of particle surface area and particle reactivity. Inhal Inhal Toxicol 19:849–856.

Fedoroff S, Richardson A. 1997. Protocols for Neural Cell Culture. Totowa, NJ:Humana Press.

Feeney CJ, Frantseva MV, Carlen PL, Pennefather PS, Shulyakova N, Shniffer C, et al. 2008. Vulnerability of glial cells to hydrogen peroxide in cultured hippocampal slices. Brain Res 1198:1–15.

Geiser M, Casailta M, Kupferschmid V, Schulz H, Semmler-Behnke M, Kreyling W. 2008. The role of macrophages in the clearance of inhaled ultrafine titanium dioxide particles. Am J Respir Cell Mol Biol 38:371–376.

Gries B, Prakash LJ. 2007. Acute Inhalation Toxicity by Contact Corrosion—the Case of WC-Co. Available: http://www.hcstarck.com/medien/tci_ampersint_map/downloads/filename_acute_inhalation_1007.pdf [accessed 23 February 2009].

Hoet PMH, Roesems G, Demedts MG, Nemery B. 2002. Activation of the hexose monophosphate shunt in rat type II pneumocytes as an early marker of oxidative stress caused by cobalt particles. Arch Toxicol 76:1–7.

IARC (International Agency for Research on Cancer). 2006. Cobalt in Hard Metals and Cobalt Sulfate, Gallium Arsenide, Indium Phosphide and Vanadium Pentoxide. IARC Monogr Eval Carcinog Risks Hum 2006;86:1–29.

Kasten U, Mullenders LH, Hartwig A. 1997. Cobalt(II) inhibits the incision and the polymerization step of nucleotide excision repair in human fibroblasts. Mutat Res 383:81–90.

Kreyling WG, Semmler M, Erbe F, Mayer P, Takenaka S, Schulz H, et al. 2002. Translocation of ultrafine insoluble iridium particles from lung epithelium to extrapulmonary organs is size dependent but very low. J Toxicol Environ Health A 65:1513–1530.

Lasfargues G, Lison D, Maldague P, Lauwerys R. 1992. Comparative study of the acute lung toxicity of pure cobalt powder and cobalt-tungsten carbide mixture in rat. Toxicol Appl Pharmacol 112:41–50.

Limbach LK, Li Y, Grass RN, Brunner TJ, Hintermann MA, Muller M, et al. 2005. Oxide nanoparticle uptake in human lung fibroblasts: effects of particle size, agglomeration, and diffusion at low concentrations. Environ Sci Technol 39:9370–9376.

Limbach LK, Wick P, Manser P, Grass RN, Bruinink A, Stark WJ. 2007. Exposure of engineered nanoparticles to human lung epithelial cells: influence of chemical composition and catalytic activity on oxidative stress. Environ Sci Technol 41:4158–4163.

Lison D. 1996. Human toxicity of cobalt-containing dust and experimental studies on the mechainism of interstitial lung disease (hard metal disease). Crit Rev Toxicol 26:585–616.

Lison D, Carbonnelle P, Mollo L, Lauwerys R, Fubini B. 1995. Physicochemical mechanism of the interaction between cobalt metal and carbide particles to generate toxic activated oxygen species. Chem Res Toxicol 8:600–606.

Lison D, De Boeck M, Verougstraete V, Kirsch-Volders M. 2001. Update on the genotoxicity and carcinogenicity of cobalt compounds. Occup Environ Med 58:619–625.

Lison D, Lauwerys R. 1990. In vitro cytotoxic effects of cobalt-containing dusts on mouse peritoneal and rat alveolar macrophages. Environ Res 52:187–198.

Lison D, Lauwerys R. 1992. Study of the mechanism responsible for the elective toxicity of tungsten carbide-cobalt powder toward macrophages. Toxicol Lett 60:203–210.

Lombaert N, de Boeck M, Decodier I, Cundari E, Lison D, Kirsch-Volders M. 2004. Evaluation of the apoptogenic potential of hard metal dust (WC-Co), tungsten carbide and metallic cobalt. Toxicol Lett 154:23–34.

Lombaert N, Lison D, van Hummelen P, Kirsch-Volders M. 2008. In vitro expression of hard metal dust (WC-Co) responsive genes in human peripheral blood mononucleated cells. Toxicol Appl Pharmacol 227:299–312.

Long TC, Saleh N, Tilton RD, Lowry GV, Veronesi B. 2006. Titanium dioxide (P25) produces reactive oxygen species in immortalized brain microglia (BV2): implications for nanoparticle neurotoxicity. Environ Sci Technol 40:4346–4252.

Moulin JJ, Wild P, Romazini S, Lasfargues G, Peltier A, Bozec C, et al. 1998. Lung cancer risk in hard-metal workers. Am J Epidemiol 148:241–248.

Nel A, Xia T, Mädler L, Li N. 2006. Toxic potential of materials at the nanolevel. Science 311:622–627.

Nemmar A, Hoet PH, Vanquickenborne B, Dinsdale D, Thomeer M, Hoylaerts MF, et al. 2002. Passage of inhaled particles into the blood circulation in humans. Circulation 105:411–414.

Nemmar A, Vanbilloen H, Hoylaerts MF, Hoet PH, Verbruggen A, Nemery B. 2001. Passage of intratracheally instilled ultrafine particles from the lung into the systemic circulation in hamster. Am J Respir Crit Care Med 164:1665–1668.

Oberdörster G, Oberdörster E, Oberdörster J. 2005. Nanotoxicology: an emerging discipline evolving from studies of ultrafine particles. Environ Health Perspect 113:823–839.

Peters A, Veronesi B, Calderon-Gardiduenas L, Gehr P, Chen LC, Geiser M, et al. 2006. Translocation and potential neurological effects of fine and ultrafine particles, a critical update. Part Fibre Toxicol 3:1–13.

Pisanic RT 2nd, Blackwell JD, Shubayev VI, Finones RR, Jin S. 2007. Nanotoxicity of iron oxide nanoparticle internalization in growing neurons. Biomaterials 28:2572–2581.

Schirmer K, Chan AGJ, Greenberg BM, Dixon DG, Bols NC. 1997. Methodology for demonstrating and measuring the photocytotoxicity of fluoranthene to fish cells in culture. Toxicol In vitro 11:107–119.

Schulze C, Kroll A, Lehr C-M, Schäfer UF, Becker K, Schnekenburger J, et al. 2008. Not ready to use—overcoming pitfalls when dispersing nanoparticles in physiological media. Nanotoxicology 2:51–61.

Stearns RC, Paulauskis JD, Godleski JJ. 2001. Endocytosis of ultrafine particles by A549 cells. Am J Respir Cell Mol Biol 24:108 –115.

Stefaniak AB, Abbas M, Day GA. 2008. Characterization of exposures among cemented tungsten carbide workers. Part I. Size-fractionated exposures to airborne cobalt and tungsten particles. J Exp Sci Environ Epidemiol doi:10.1038/jes.2008.37 [Online 16 July 2008].

Spurr AR. 1969. A low-viscosity epoxy resin embedding medium for electron microscopy. J Ultrastruct Res 26:31–43.

Takenaka S. Karg E, Roth C, Schulz H, Ziesenis A, Heinzmann U, et al. 2001. Pulmonary and systemic distribution of inhaled ultrafine silver particles in rats. Environ Health Perspect 109(suppl 4):547–551.

van Goethem F, Lison D, Kirsch-Volders M. 1997. Comparative evaluation of the in vitro micronucleus test and the alkaline single cell gel electrophoresis assay for the detection of DNA damaging agents: genotoxic effects of cobalt powder, tungsten carbide and cobalt-tungsten carbide. Mutat Res 392:31–43.

Wörle-Knirsch JM, Kern K, Schleh C, Adelhelm C, Feldmann C, Krug HF. 2007. Nanoparticulate vanadium oxide potentiated vanadium toxicity in human lung cells. Environ Sci Technol 41:331–336.

Zegura B, Volcic M, Lah TT, Filipič M. 2008. Different sensitivities of human colon adenocarcinoma (CaCo-2), astrocytoma (IPDDC-A2) and lymphoblastoid (NCNC) cell lines to microcystin-LR induced reactive oxygen species and DNA damage. Toxicon 52(3):518–525.

Zhang Q, Kusaka Y, Donaldson K. 2000. Comparative pulmonary responses caused by exposure to standard cobalt and ultrafine cobalt. J Occup Health 42:179–184.

Zhang Q, Kusaka Y, Zhu X, Sato K, Mo Y, Kluz T, et al. 2003. Comparative toxicity of standard nickel and ultrafine nickel in lung after intratracheal instillation. J Occup Health 45:23–30.